Enhanced Dielectric Properties of Sintered $MgFe_{1.98}Nd_{0.02}O_4$ Nanoparticles

[1,2]U. Rafiq, [1, 3]M. Hanif, [1]M. Anis-ur-Rehman and [2]A. Ul Haq[*]
[1]*Applied Thermal Physics Laboratory, Department of Physics, COMSATS University, Islamabad 44000, Pakistan*
[2]*Riphah International University, Islamabad 44000, Pakistan.*
[3]*Department of Electrical and Electronic Engineering, Universiti Teknologi Petronas, Tronoh, Malaysia.*
anwar.haq@riphah.edu.pk*

(Received on 25th September 2018, accepted in revised form 28th March 2019)

Summary: Spinal $MgFe_{1.98}Nd_{0.02}O_4$ was prepared by simplified sol-gel method. To measure the dielectric properties samples were sintered from 700-800 °C in the steps of 50 °C. The sample's phase purity, crystallographic phase and crystallite size was measured by X-ray diffraction method (XRD). The pellets were analyzed in Scanning Electron Microscope for their surface morphology and grain shape. Dielectric properties were measured from 20 Hz to 3 MHz at room temperature. Samples sintered at 750 °C, showed highest value of AC conductivity which indicated that the material is suitable for use in sensors. However, minimum value of dielectric loss factor was obtained at 800 °C which makes it more suitable for antenna applications.

Key words: Dielectric conductivity, High-frequency applications, Rare earths, Sintering temperature.

Introduction

If certain metal oxides and an oxide of iron (which have two unequal sublattices and are ordered anti-parallel to each other) are alloyed than product is termed as ferrites and possesses ferrimagnetic properties. Each sublattice may be magnetized spontaneously at room temperature [1-6]. They have been widely investigated to extend their domain of applications in electronics e.g. memory cores, magnetic media, gas sensors, high frequency devices, catalysis, etc. [7] Among various ferrites, the magnesium ferrite ($MgFe_2O_4$) is unique due to its low eddy currents and high resistivity values and as a result being used in hyperthermia, sensors, catalysis, adsorption, recording media, and magnetic technologies. Nano particles of $MgFe_2O_4$ have also better photo electrical properties [1, 7-11].

Various chemical and physical methods are reported in the literature for the synthesis of Mg ferrites such as citrate method [12, 13], chemical method [14-16], co-precipitation method, [17-19], combustion method [15, 20, 21], High temperature thermal decomposition [22], Electro-spinning [23], solid-state reaction method [22, 24], hydrothermal method [25], sol–gel method [15, 22, 26-28] etc. Among above mentioned routes, Sol-gel method is known to produce most outstanding results for the synthesis of phase pure particles of nanometer size at relatively low temperature.

Effect of small percentages of metal ion substitution such as Al [29, 30], Ca [31], Co [32], Cr [33], Cu [34], Ge [35], Ni [36], Mo and Sn [37], Si [38] and Zn [39] on structure, dielectric and magnetic behavior of $MgFe_2O_4$ have been reported. However, not much published work is available on doping of rare earth elements in the $MgFe_2O_4$ and their electrical or magnetic properties. Bamzai *et al* [40] prepared Dysprosium Dy^{3+} doped Magnesium ferrite, $MgDy_xFe_{2-x}O_4$ (x=0.00 to 0.07). They used solid state method to prepare the material and measured its magnetic properties. Kumar *et al* [41] prepared $MgGd_{0.15}Fe_{1.85}O_4$ ferrite with improved magnetic and electrical properties by solid state reaction technique and reported their microstructures, magnetic and electrical properties. It is reported that substitution of rare earth ions produce strains into the spinel structure. Similarly, Manikandan *et. al*. [42-45] reported rare earth element doped cobalt ferrite and its opto-magnetic properties. Anu Rana *et. al*. [46] reported that dielectric parameters of Gd doped cobalt ferrite are strongly dependent upon Gd^{3+} ion concentrations and their frequency dependence. Recently, the dielectric properties such as AC conductivity, dielectric loss factor, dielectric constant and tangent loss as a function of Nd concentration on the phase pure Mg ferrite has been reported [28]. Some of these results not reported (Fig. 1) earlier are presented here. The Fig. shows that the values of dielectric constant (Fig 1a), dielectric loss factor (Fig 1b) and AC conductivity (Fig 1c) as a function of Nd concentration follow similar trend. However, Tangent loss shows sharp decrease as a function of Nd concentration up to 0.02% Nd concentration. Further increase in the concentration of Nd doping showed increase in the tangent loss values. Thus minimum

[*]**To whom all correspondence should be addressed.**

value of tangent loss is seen at 0.02% of Nd [28]. This indicates that this material is suitable for the sensing devices of perfect vacuum, dry air and most pure gases such as helium, nitrogen and energy efficient devices. It is generally known that factors such as sintering temperature, rate of heating, sintering time, rate of cooling, etc. [4] strongly influence the physical and chemical properties of ferrites. Therefore it was considered worthwhile to investigate and report the dielectric properties dependence of $MgFe_{1.98}Nd_{0.02}O_4$ on sintering temperature in the range of 700 to 800 °C.

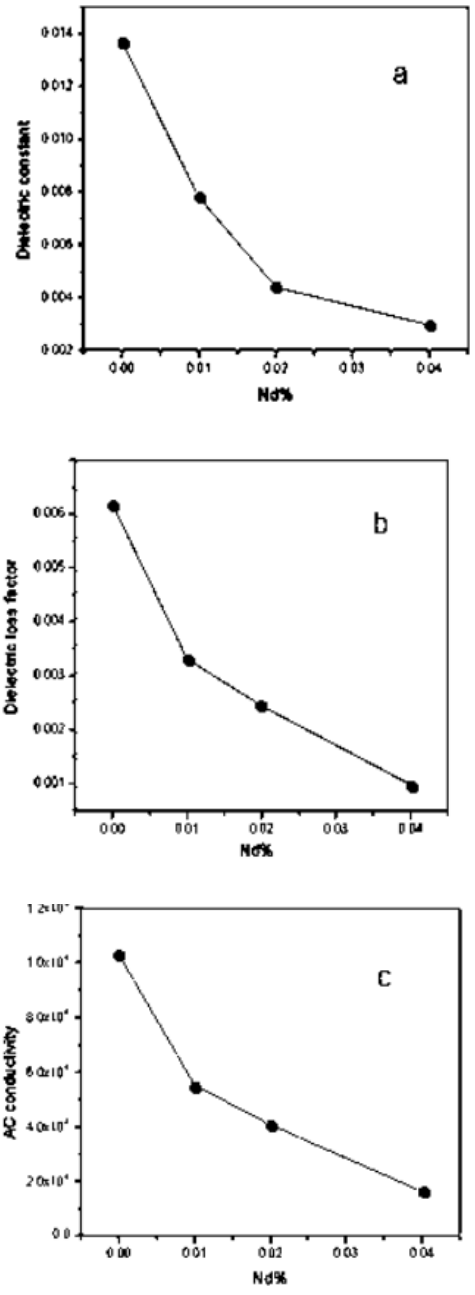

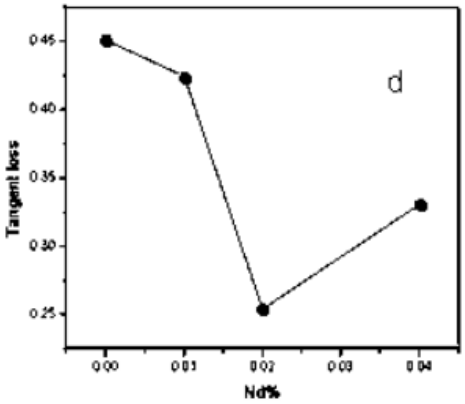

Fig. 1: Dielectric constant (a), Dielectric loss factor (b) and AC conductivity (c) and Tangent loss (d) as a function of Nd doping in Magnesium Ferrite at constant frequency of 100 Hz.

Experimental

Simplified sol-gel method was used to prepare the Neodymium based Magnesium ferrite, $MgFe_{1.98}Nd_{0.02}O_4$ [28]. The analytical grade magnesium nitrate, iron nitrate and neodymium nitrate were weighed in the stoichiometric ratio and dissolved in the ethylene glycol separately. The salts and ethylene glycol were taken in the molar ratio of 1:14. The homogeneous solution was obtained after continuous stirring of 30 minutes at room temperature. Than the solutions were mixed and temperature of solution was gradually raised to 80 ◦C. The continuous stirring resulted thick gel formation. The temperature was further increased to 320 ◦C; mixture caught fire and started burning. When flames were extinguished, the product appeared as brown powder. To perform characterizations, the powder was pressed in to pallets. All the pallets (samples) were sintered in a Protherm furnace (model PLF 110/6) for two hours at selected temperatures. The samples were studied for the structural analysis and phase purity by X-ray diffraction (XRD) technique. XRD spectrums were recorded using Cu-Kα radiations (λ = 1.5406 A°) from 20◦ to 80◦. XRD patterns were recorded from PANalytical X'Pert Pro (MPD) diffractometer. The operating voltage was 40 keV and 30 mA. Ni filter was used to get Cu-Kα radiation. Lattice parameters were calculated using software called "CheckCell". A FESEM of HITACHI SU-1500 was used to study the surface morphology and grain size of the samples. A LCR Analyzer made by Wayne Kerr (Model 6440B) was used to measure frequency dependence of the dielectric properties in the range of 20 Hz to 3 MHz at room temperature for all sintered pallets by two probe methods. Pressure contacts were of the size of the pallet. To achieve better contacts polished

surface of the pallet was used. The dissipation factor (tan*δ)* is found by dividing the energy dissipated by the energy stored in the component. Values of the dielectric constant were calculated using the equation [19]:

$\varepsilon = Cd/ \varepsilon_0 A$

where pallet's cross-sectional area is A, thickness is d, capacitance is C and permittivity of free space is ε_0. Dielectric loss factor (ε') related to the complex relative permittivity, ε' is a measure of the loss of energy in the dielectric material through conduction, slow polarization currents and other dissipative phenomena.

The values of dielectric loss tangent, (tan δ) and dielectric constant (έ) at the same frequency range can be used to calculate the AC conductivity by using the following relation [46]:

$$\sigma_{AC} = \omega \varepsilon_0 \acute{\varepsilon} \tan(\delta).$$

where σ_{AC} is the AC conductivity and ω is the angular frequency.

Results and Discussion

XRD patterns for the samples are shown in Fig. 2 at different sintering temperatures. Well defined diffraction peaks and respective peak intensities are increasing with the increase of sintering temperature. All the peaks match with the JCPD card no 01-088-1937 and indexed accordingly for the cubic lattice. Maximum intensity peak in this pattern is (311). Table-1 shows the increase in the crystallite size as a function of sintering temperature. The values of lattice constant are not dependent upon sintering temperature and are not statistically significant. This is in confirmation with the work of Ilhan *et. al*. [17], Omer *et. al*. [48] and Gabal *et. al* [49].

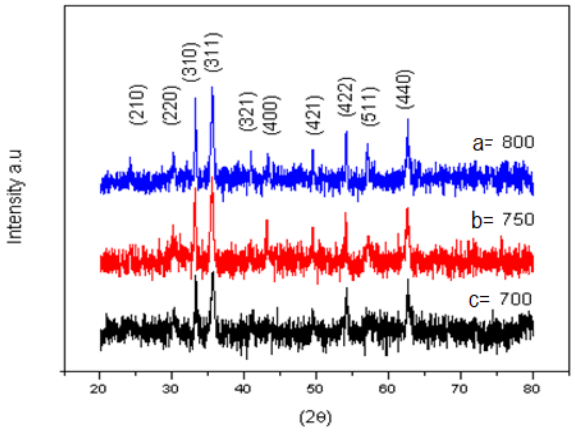

Fig. 2: XRD pattern of $MgFe_{1.98}Nd_{0.02}O_4$ as a function of sintering temperature.

The grain structure and surface morphology of Nd doped magnesium ferrite as a function of sintering temperature was studied in a FE-SEM and is shown in Fig.3. The grain size in all micrograpghs ranges from 100-500 nm. The average value of the grain size is 250 ± 100 nm. It was concluded that substitution of neodymium restricts the grain growth.

Table-1: The changes in the values of average crystallite size and lattice parameter as function of sintering temperature.

Sintering temperatures (°C)	Crystallite size(nm)	Lattice parameter(Å)
700	**23 ± 3**	**8.38±0.07**
750°C	**27 ± 3**	**8.39±0.08**
800°C	**37 ± 4**	**8.36±0.08**

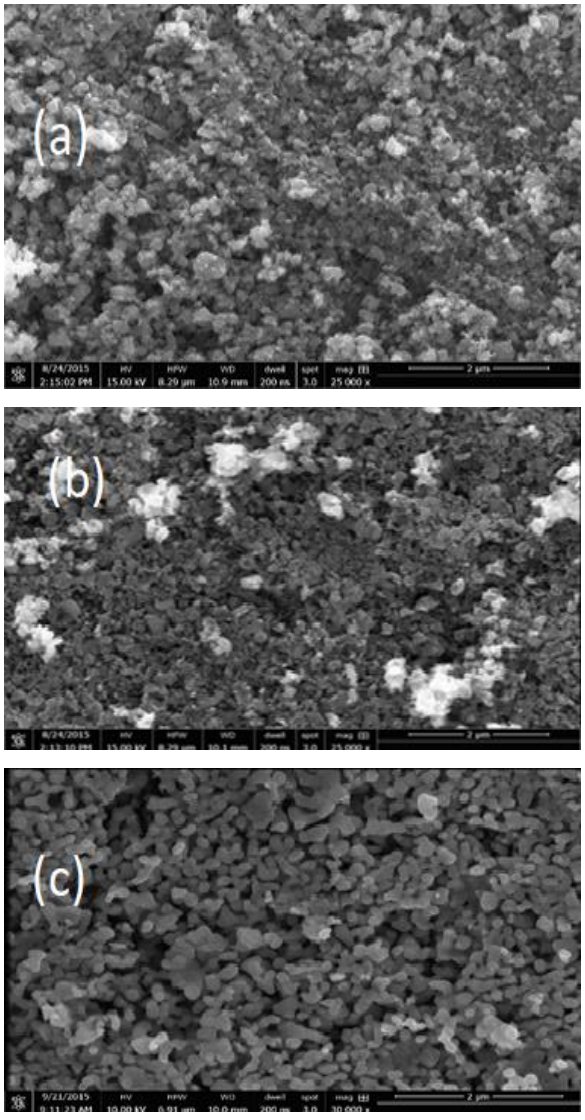

Fig. 3: Micro structure of samples sintered at (a) 700 oC, (b) – 750 oC and (c) -800°C for $MgFe_{2-x}Nd_xO4(x=0.02)$.

Fig.4a presents the changes in the values of dielectric constant with the sintering temperature. Two distinct regions may be seen in this Fig. First region lies in between 10^2-10^3 Hz and second region is located from 10^3-10^6 Hz. The first region marks decrease in the values of dielectric constant with the increase in frequency because charge carriers are aligned along the direction of the applied field to produce a high dielectric constant value. This leads to decrease in the values of dielectric constant at higher frequencies. But in second region the dielectric constant remains almost constant and is independent of the frequency due to the reason that charge carriers cannot orient themselves along the applied field direction. This is the reason that the graph becomes constant at higher frequencies [12].

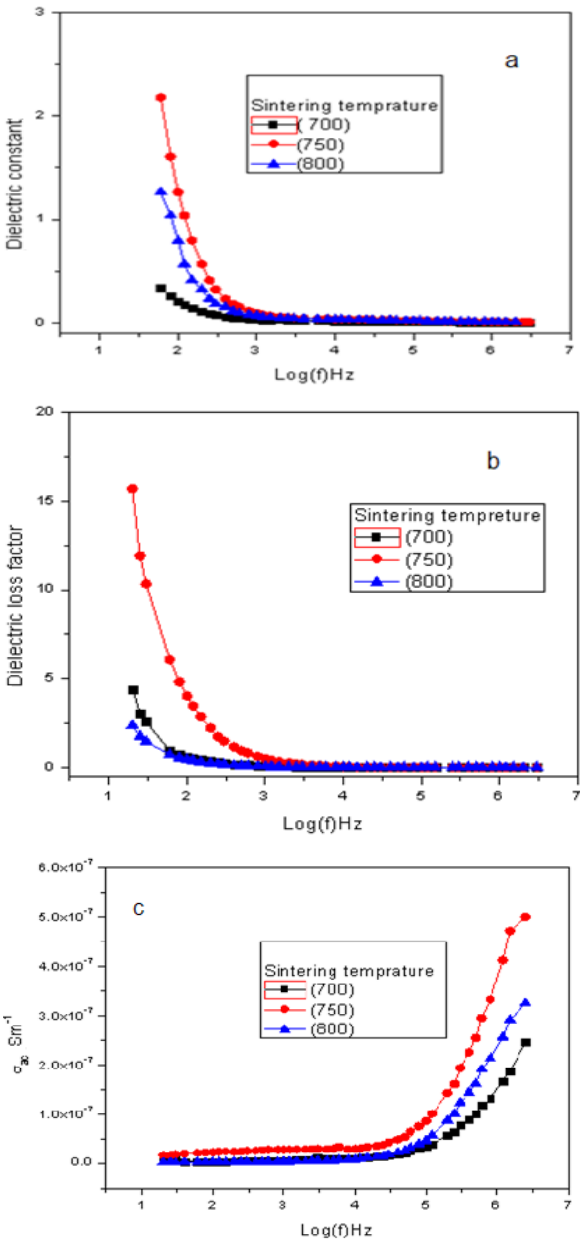

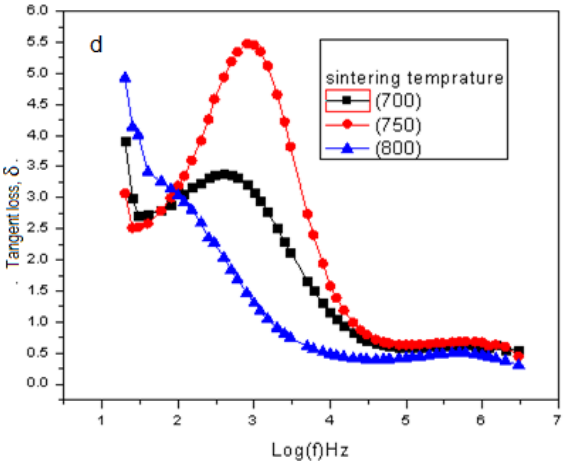

Fig. 4: Effect of sintering temperature on dielectric properties as a function of frequency. (a) Dielectric loss (b) Dielectric loss factor (c) AC electrical conductivity δ AC and (d) Tangent loss δ for sintered samples.

It is remarkable to mention that at low frequency (60 Hz), the value of dielectric constant has increased with the increase in the sintering temperature. This shows a direct relationship between dielectric constant and the sintering temperature due to the space charge polarization, electrons displacement and the charge produced at the insulating grain boundaries. The partial reduction of Fe^{3+} to the Fe^{2+}ions is the cause of the increase of dielectric constant values due to increase in sintering temperature. The minimum dielectric constant is observed at 700 °C because of less contribution of Fe^{2+} ions and decrease in the space charge polarization expected at this temperature in the ferrites [41, 50].

Fig.4b shows the dielectric loss factor as a result of sintering and consists of two regions. The frequency range 10 to 10^2 Hz defines first region whereas second region lies between $10^{2.5}$ to$10^{6.5}$ Hz. The dielectric loss factor has sharply decreased in the first region because the required energy is available to align the localized dipoles in the field direction. But in the second region, energy is not sufficient to orientate dipoles in the applied field direction. That's why in high frequency region, the values of dielectric loss factor does not change and remains almost constant [21]. The values of dielectric loss factor have increased with the increase in the values of sintering temperature. At sintering temperature of 800 °C the loss factor of the sample is smaller than the sample sintered at 700 and 750°C due to the increase in grains size and reduction of number of Fe^{3+} ions which transforms into to Fe^{2+}ions [41].

The AC conductivity of sintered $MgFe_{1.98}Nd_{0.2}O_4$ is shown in Fig.4c. This plot may also be divided in two regions. The first region is located between 10 to10^4 Hz. The second region starts from 10^5 to $10^{6.5}$Hz. In the first region the AC conductivity of ferrite remains constant up to 10^4 Hz because at the lower frequencies grain boundary contributes in AC conductivity and low electrons jumping frequency among the metal ions of adjustable valence states. Thus AC conductivity is low at lower frequencies. However, the AC conductivity has sharply increased in the second region above 10^5 Hz. This is due to the reason that at higher frequencies grain boundaries have contributed in the AC conductivity. When the frequency is increased, the active grain boundaries restrict the electrons to hope among the matching metal ions of adjustable valence states. So AC conductivity increased with increasing in frequency values [41]. The AC conductivity changed with the sintering temperature. Increase in AC conductivity is dependent upon the microstructural features and also conversion of trivalent Fe^{3+} ions to Fe^{2+}state. The crystallite size is increasing with the increase in the sintering temperature which resulted diffusion of grain boundaries in turn and leads to increase the AC conductivity.

Dependence of Tangent loss as a function of frequency shows fascinating results. Four regions may be seen in Fig.4d. The first region occurs between 60 to $10^{1.5}$ Hz. The range of second region is 10^2 to $10^{2.8}$ Hz. The third region lies between 10^3 to 10^5 Hz and fourth region is above 10^5 Hz. The Tangent loss decreased in the first and third region, because the energy is sufficient to restrict the dipoles to orientate them in the direction of the applied field. In second region Tangent loss has increased due to the insufficient energy to restrict dipoles. In the fourth region values of Tangent loss has remained constant because polarization has reduced with aggregation of frequency and became constant because external field frequency cannot follow the alternating field. Loss tangent is changing with the sintering temperature. Thus it may be concluded that the value of dielectric loss is highest at 750 ^oC as compared to the other samples sintered at 700 and 800 ^oC, because period of relaxation process is similar as that of applied field at this temperature. When the relaxation time is more than the duration of the applied field, losses are small. This is the reason that dielectric losses at 800^oC are minimal [28].

Conclusions

The measurement of tangent loss (δ) of the magnesium ferrite as a function of Nd doping (Fig 1d) shows that the values tangent loss of $MgFe_{1.98}Nd_{0.02}O_4$ are about 50% less as compared to the other Nd doped ($MgFe_{2-x}Nd_xO_4$, x=0.00, 0.01, 0.04) samples. It may be due to the improvement in the microstructure of the material. This makes the material suitable for use at high frequency applications. To make more reliable the dielectric properties of the sample $MgFe_{1.98}Nd_{0.02}O_4$ is studied as a function of sintering temperatures between 700 to 800°C. The samples showed very motivating results. One of them is enormous reduction in the values of the tangent loss observed at 800°C. Maximum AC conductivity is achieved at 750 °C but above 750°C the AC conductivity decreased rapidly so we assume that 750°C is the optimum sintering temperature to achieve minimum tangent loss values.

References

1. A. M. Duncan, H. D. Rouvaray, Microclusters, Scientific American, 110 (1989).
2. A. P. Subramanian, S. K. Jaganathan, A. Manikandan, K. N. Pandiaraj, Gomathi Nd and E. Supriyanto, Recent trends in nano-based drug delivery systems for efficient delivery of phytochemicals in chemotherapy, *RSC Advances* **6** 48294 (2016).
3. Abraham A. Godlyn, A. Manikandan, E. Manikandan, S. K. Jaganathan, A. Baykal and P. Sri Renganathan; Enhanced Opto-Magneto Properties of $Ni_xMg_{1-x}Fe_2O_4(0.0 \leq x \leq 1.0)$ Ferrites Nano-Catalysts; *Journal of Nanoelectronics and Optoelectronics* **12** 1326 (2017)
4. E. Hema, A. Manikandan, P. Karthika, M. Durka, S. Arul Antony and B.R. Venkatraman; Magneto-Optical Properties of Reusable Spinel $Ni_xMg_{1-x}Fe_2O_4(0.0 \leq x \leq 1.0)$ Nano-Catalysts; *Journal of Nanoscience and Nanotechnology* **16** 7325 (2016).
5. K Reena Chitra,, A Manikandan and S Arul Antony; Antibacterial Studies and Effect of Poloxamer on Gold Nanoparticles by Zingiber Officinale Extracted Green Synthesis *Journal of nanoscience and nanotechnology* **15**, 4984 (2015)
6. Boominathan Meenatchi, Velayutham Renuga and Ayyar Manikandan; Size-controlled synthesis of chalcogen and chalcogenide nanoparticles using protic ionic liquids with imidazolium cation; *Korean Journal of Chemical Engineering* **33**, 934 (2016).
7. M. Sugimoto, The past, present, and future of ferrites, *J. American Ceramic Society*, **82**, 269 (1999)

8. A. Manikandan, M. Durka, M. Amutha Selvi andS. Arul Antony; Sesamum indicum Plant Extracted Microwave Combustion Synthesis and Opto-Magnetic Properties of Spinel MnxCo1-xAl2O4 Nano-Catalysts*; Journal of nanoscience and nanotechnology* **16**, 448 (2016).
9. Y. Slimani , A. Baykal - Imam Abdulrahman and A. Manikandan; Effect of $Cr3^{+}$ substitution on AC susceptibility of Bahexaferrite nanoparticles; *Journal of Magnetism and Magnetic Materials* **458**, 204 (2018)
10. A. Mary Jacintha, A. Manikandan, K. Chinnaraj, S. Arul Antony and P. Neeraja; Comparative Studies of Spinel $MnFe_2O_4$ Nanostructures: Structural, Morphological, Optical, Magnetic and Catalytic Properties; *Journal of nanoscience and nanotechnology* **15**, 9732 (2015).
11. D. Maruthamani, S. Vadivel, M. Kumaravel, B. Saravanakumar, B. Paul, S. S. Dhar, A. Habibi-Yangjeh, A. Manikandan and G. Ramadoss; Fine cutting edge shaped Bi_2O_3rods/reduced graphene oxide (RGO) composite for supercapacitor and visible-light photocatalytic applications; *Journal of colloid and interface science* **498**, 449 (2017).
12. R. Sepahv, R. Mohamadzade, Synthesis and characterization of carbon nanotubes decorated with Magnesium Ferrite (MgFe2O4) nanoparticles by citrate-gel method, *J. Sciences, Islamic Republic of Iran* 22(2) (2011), 177-182
13. I.V. Kasi Viswanath, Y.L.N. Murthy, Kondala Rao Tata, Rajendra Singh, Synthesis and characterization of Nano Ferrites by citrate gel method, Int. J. Chem. Sci., **11**, 64 (2013).
14. N.M. Deraz, O.H. Abd-Elkade, Effects of Magnesia content on spinel Magnesium Ferrite formation, *Int. J. Electrochem. Sci.*, **8**, 8632 (2013).
15. Sheikh Manjura Hoque, M. Abdul Hakim, Al Mamun, Shireen Akhter, Md. Tanvir Hasan, Deba Prasad Paul, Kamanio Chattopadhayay, Study of the bulk magnetic and electrical properties of MgFe2O4 synthesized by chemical method, *Materials Sciences and Applications*, **2**, 1564 (2011).
16. Navneet Kaur, Manpreet Kaur, Comparative studies on impact of synthesis methods on structural and magnetic properties of magnesium ferrite nanoparticles, Processing and Application of Ceramics **8**, 137 (2014).
17. S. Ilhan, S. G. Izotova, A.A. Komlev, Synthesis and characterization of $MgFe_2O_4$ nanoparticles prepared by hydrothermal decomposition of co-precipitated magnesium and iron hydroxides. Ceramics International, **41**, 577 (2015)
18. Y. Shi, J. Ding, X. Liu and J. Wang, $NiFe_2O_4$ ultrafine particles prepared by co-precipitation/ mechanical alloying, J. of Magnetism and Magnetic Materials, **205**, 249 (1999)
19. M Yasin Shami, MS Awan, M. Anis-ur-Rehman, Phase pure synthesis of $BiFeO_3$ nanopowders using diverse precursor via co-precipitation method, J. Alloys Compd. **509**, 10139 (2011).
20. V. Sachin. D. R. Bangale, S. Patil, R. Bamane, Preparation and electrical properties of nanocrystalline $MgFe_2O_4$ oxide by combustion route, Archives of Applied Science Research, **3**, 506 (2011).
21. Smitha Thankachan, Manju Kurian, Divya S Nair, Sheena Xavier, E.M. Mohammed, Effect of rare earth doping on structural, magnetic, electrical properties of magnesium ferrite and its catalytic activity, International Journal of Engineering Science and Innovative Technology (IJESIT) **3**, 529 (2014).
22. X. Sung Wook Hyun, Hyung Joon Kim, Chu Sik Park, Kyoung-Soo Kang, Chul Sung Kim, Synthesis and size dependent properties of Magnesium Ferrites, IEEE Transactions on Magnetics, **45**, 2551 (2009).
23. Santi Maensiri, Montana Sangmanee, Amporn Wiengmoon, Magnesium Ferrite (3gFe2O4) nanostructures fabricated by electrospinning, Nanoscale Res Lett **4**, 221 (2009).
24. M. Kaur, B.S. Randhawa, P.S. Tarsikka, Synthesis of $Mg_{0.3}Zn_{0.7}Fe_2O_4$ nanoparticles from thermolysis of magnesium zinc tris maleatoferrate (III) heptahydrate, Ind. J. Eng. Mater. Sci., **20**, 325 (2013).
25. W.L. Suchanek, R.E. Riman, Hydrothermal synthesis of advanced ceramic powders, Adv. Sci. Technol., **45**, 184 (2006)
26. S.I. Hussein, A.S. Elkady, M.M. Rashad, A.G. Mostafa, R.M. Megahid, Structural and magnetic properties of magnesium ferrite nanoparticles prepared via EDTA-based sol–gel reaction. J. Magnetism and Magnetic Materials, **379**,.9 (2015)
27. Franco Jr., M.S. Silva High temperature magnetic properties of magnesium ferrite nanoparticles, J Applied Physics **109**, 7 (2011).
28. U. Rafiq, M. Hanif, M. Anis-ur-Rehman, A. ul Haq, J Supercond Nov Magn **30**, 3559 (2017).
29. K.S. Kim, S.H. Han, H.G. Kim, Magnetic and structural properties of $MgFe_{2-x}Al_xO_4$ *Journal of the Korean Physical Society* **54**, 886 (2009).
30. Shahzad Hossain, Mohammad Kamrul Hasan, S.K. Md. Yunus, A.K.M. Zakaria, Tapash Kumar Datta, Abul Kalam Azad, Synthesis and investigation of the structural properties of Al^{3+} doped Mg Ferrites, Applied Mechanics and Materials, **789-790**, 48 (2015).

31. K.K. Bamzai, Gurbinder Kour, Balwinder Kaur, S.D. Kulkarni, Preparation, and Structural and Magnetic Properties of Ca substituted Magnesium Ferrite with composition MgCaxFe2−xO4 (= 0.00, 0.01, 0.03, 0.05, 0.07,) Journal of Materials Article ID 184340 (2014), http://dx.doi.org/10.1155/2014/184340
32. S.M. Kadam, B.M. Kulkarni, B.K. Chougule, On the nature of electrical resistivity in Co-Mg Ferrites., J Shivaji University (Science & Technology) **41**, 1 (2014-15).
33. M. Raghasudha, D. Ravinder, P. Veerasomaiah, Electrical resistivity studies of Cr doped Mg nano-ferrites, Materials Discovery, 2 (2015), 50-54
34. J. Saranya, M. Balavijayalakshmi, Synthesis and Characterization of copper doped Magnesium Ferrite nanoparticles, J. Nanoscience and Nanotechnology **2**, 397 (2014).
35. D.R. Sagar, C. Prakash, P. Kishan, Cation distribution in germanium-substituted magnesium ferrites, *Solid State Communications* **68**, 193 (1988).
36. Mahbubul Haque, Hanium Maria Kazi, Shamima Choudhury, Mahabub Alam Bhuiyan, M.A. Hakim, Synthesis, microstructure and magnetic properties of Ni-Mg ferrites, J Ceramic Processing Research. **14**, 82 (2013).
37. C. Doroftei, E. Rezlescu, N. Rezlescu, P. D. Popa, Magnesium ferrite with Sn^{4+} and / or Mo^{6+} substitutions as sensing element for acetone and ethanol, Rom. J Phys **51**, 631 (2006).
38. [38] Akane Doi, Maiko Nishibori, Kenji Obata, Takuya Suzuki, Kengo Shimanoe, Shigenori Matsushima, Micronization of $MgFe_2O_4$ particles doped with Si, J Ceramic Society of Japan 124(7) (2016) , 777
39. S.S. Khot, N.S., Shinde, B.P. Ladgaonkar, B.B. Kale, S.C. Watawe, Magnetic and structural properties of Magnesium Zinc Ferrites synthesized at different temperature, *Adv. Applied Science Research*: **2** 460 (2011).
40. K.K. Bamzai, G. Kour, B. Kaur, S.D. Kulkarni, Effect of cation distribution on structural and magnetic properties of Dy substituted magnesium ferrite, *Journal of Magnetism and Magnetic Materials*, **327**, 159 (2013).
41. J. Chand, G. Kumar, P. Kumar, S.K. Sharma, M. Knobel, M. Singh, Effect of Gd^{3+} doping on magnetic, electric and dielectric properties of $MgGd_xFe_{2-x}O_4$ ferrites processed by solid state reaction technique. *J Alloys and Compounds*, **509**, 9638 (2011).
42. K. Elayakumar, A. Manikandan, A. Dinesh, K. Thanrasu, K. Kanmani Raja, R. Thilak Kuman, Y. Slimani, S. K. Jaganathan and A. Baykal; Enhanced magnetic property and antibacterial biomedical activity of Ce3+ doped CuFe2O4 spinel nanoparticles synthesized by sol-gel method; *Journal of Magnetism and Magnetic Materials* (2019).
43. A. Manikandan, J. Judith Vijaya, M. Sundararajan, C. Meganathan, L. John Kennedy and M. Bououdina; Optical and magnetic properties of Mg-doped $ZnFe_2O_4$ nanoparticles prepared by rapid microwave combustion method; Superlattices and Microstructures **64**, 118 (2013).
44. A. Manikandan, L. John Kennedy, M. Bououdina and J. Judith Vijaya; Synthesis, optical and magnetic properties of pure and Co-doped $ZnFe_2O_4$ nanoparticles by microwave combustion method; *Journal of Magnetism and Magnetic Materials* **349**, 249 (2014).
45. A. Manikandan, M. Durka, K. Seevakan and S. Arul Antony; A Novel One-Pot Combustion Synthesis and Opto-magnetic Properties of Magnetically Separable Spinel $Mn_xMg_{1-x}Fe_2O_4$ ($0.0 \leq x \leq 0.5$) Nanophotocatalysts; *Journal of Superconductivity and Novel Magnetism* **28**, 1405 (2015).
46. Anu Rana, O.P. Thakur, Vinod Kumar, Effect of Gd^{3+} substitution on dielectric properties of nano cobalt ferrite, *Material letters*, **65**, 3191 (2011)
47. S. Nasir, G. Asghar, M.A. Malik, M. Anis-ur-Rehman, Structural, dielectric and electrical properties of zinc doped nickel nanoferrites prepared by simplified sol–gel method, *J. Sol-gel Sci. Techn.*, **59**, 111 (2011).
48. M.I. Omer, A.A. Elbadawi, and O.A. Yassin, Synthesis and Structural Properties of Fe_2O_4 Ferrite Nano-particles. *J Appl Ind Sci*, **1**, 2328 (2013).
49. M.A. Gabal, A.M. Abdel-Daiem, Y.M. Al Angari, I.M. Ismail, Influence of Al-substitution on structural, electrical and magnetic properties of Mn–Zn ferrites nanopowders prepared via the sol–gel auto-combustion method. *Polyhedron*, **57**, 105 (2013).
50. G. Kumar, J. Shah, R.K. Kotnala, V.P. Singh, M. Dhiman, S.E. Shirsath, M. Singh, Remarkable magnetization with ultra-low loss $BaGd_xFe_{12-x}O_{19}$ nanohexaferrites for applications up to C-band, *J Magnetism and Magnetic Materials*, **390**, 50 (2015).